

# Kinetics of three-dimensional Langmuir collapse

V. E. Zakharov, A. N. Pushkarev, A. M. Rubenchik, R. Z. Sagdeev, and V. F. Shvets

*Scientific Consul on Cybernetics Problems, USSR Academy of Sciences*

(Submitted 17 March 1989)

Zh. Eksp. Teor. Fiz. **96**, 591–603 (August 1989)

The final stage of evolution of a three-dimensional Langmuir caviton is investigated by particle simulation. A clear picture of collapse is obtained. The main characteristics of the caviton and its interaction with electrons differ significantly from the analogous quantities obtained in two-dimensional calculations. The large minimum size of the caviton ( $\sim 16 r_D$ ) and its degree of anisotropy are in agreement with those obtained experimentally. The burnout of the very intense structures is accompanied by the formation of vortices in phase space and multiflows, and the expulsion of an appreciable number of particles from the caviton.

## 1. INTRODUCTION

The phenomenon of the collapse of Langmuir waves predicted theoretically<sup>1</sup> in 1972 and recently verified experimentally<sup>2</sup> has a fundamental significance for contemporary plasma physics. Specifically, collapse, the formation in plasma of catastrophically deepening regions of lower density containing trapped Langmuir waves, is the basic collisionless mechanism for dissipation of wave energy. It is also the natural structural element of strong Langmuir turbulence both in space and laboratory plasmas. For more than 15 years collapse of Langmuir cavitons has been subjected to intense analytic and numerical study (see the reviews<sup>3–6</sup> and the literature cited in them; the latest papers are Refs. 7–16). It should be noted that beginning with Ref. 1, wave collapse became a generally accepted concept of contemporary physics: possibilities are various types of self-focused quasi-monochromatic waves, collapse of electromagnetic and lower hybrid waves, and other forms of wave collapse.<sup>17</sup>

The general picture of Langmuir collapse now has the following general features. Cavitons are formed in turbulent plasma filled with oscillations as a result of the development of the modulational instability. The initial energy density in the caviton  $W$  is of the order of the average turbulence level  $W_0$  and the characteristic size of the caviton  $1 \sim r_D (nT/W)^{1/2}$ . The process of caviton compression quickly enters the self-similar regime and the caviton takes on a universal significantly oblate form. During the collapse the energy of oscillations trapped in the caviton is conserved. In the final stage wave-particle interactions become important and the oscillations trapped in the caviton burn out, accelerating the plasma electrons. As a result the energy is transferred to a small group of fast particles.

Right up to the final evolutionary stage the caviton is described by a system of dynamic equations averaged over the fast time obtained using a hydrodynamic description of the plasma<sup>1</sup>:

$$\Delta(2i\psi + 3\omega_p r_D^2 \Delta\psi) = \frac{\omega_p}{n_0} \nabla(\delta n \nabla\psi), \quad (1a)$$

$$\delta\ddot{n} - c_s^2 \Delta\delta n = -\Delta \frac{|\nabla\psi|^2}{16\pi M}. \quad (1b)$$

Here  $\Psi$  is the average potential of the high frequency field

$$\mathbf{E} = \nabla[\psi \exp(-i\omega_p t) + \text{c.c.}]/2,$$

and  $\delta n$  is the quasi-neutral variation of the plasma density.

These equations conserve the following integrals of motion: number of quanta

$$N = \int |\nabla\psi|^2 d\mathbf{r} \quad (2)$$

and Hamiltonian

$$H = \int \left[ \frac{3r_D^2}{16\pi} |\Delta\psi|^2 + \frac{\delta n}{16\pi n_0} |\nabla\psi|^2 + Mn_0 \frac{v^2}{2} + \frac{Mc_s^2}{2n_0} (\delta n)^2 \right] d\mathbf{r} \quad (3)$$

and have collapsing solutions in two- and three-dimensional problems. The most important properties of Langmuir collapse in the inertial range follow from Eqs. (1) in dimensionalities  $d = 2, 3$ . A sufficient condition for collapse is for the Hamiltonian to be negative, which is too strong a condition in the three-dimensional case where collapse occurs even with initial conditions such that<sup>3</sup>

$$H < \frac{3}{16\pi} \left( \frac{r_D}{r_0} \right)^2 N, \quad (4)$$

where  $r_0$  is the characteristic size of the initial perturbation.

One can neglect the finite speed of sound in Eq. (1b) for an intensity  $W/nT > m/M$  and the collapse enters the supersonic regime. Supersonic collapse is self-similar asymptotically for  $t \rightarrow t_0$ :

$$|\mathbf{E}|^2 \propto (t_0 - t)^{-2}, \quad \frac{\delta n}{n_0} \propto (t_0 - t)^{-1/d}, \quad l \propto (t_0 - t)^{2/d}, \quad (5)$$

where  $t_0$  is the time of singularity formation.

The collapsing caviton has an isotropic oblate form with the electric field in the center of the caviton directed along its short axis. The caviton asymmetry is connected with the unrealistic character of the spherically-symmetric collapse model. In such a model the field in the center of the caviton is zero, there are no pondermotive forces, and a density hump forms at the center of coordinates. As shown by calculations a dipole charge distribution in the caviton is more realistic. Equations (1) have been repeatedly solved numerically (see the references cited in Ref. 3). The results of calculations corroborate the caviton properties listed above and, in particular, demonstrate a transition from quite arbitrary initial conditions to the self-similar regime (5).

The applicability of Eqs. (1) is limited to small levels of high frequency (HF) energy  $W/nT \ll 1$  and large caviton sizes  $kr_D \ll 1$ . Many effects not taken into account in Eq. (1) become important with caviton compression and the growth

of field intensity. First among them are the interaction of electrons with Langmuir oscillations and electron nonlinearities. Saturation of nonlinearity, change of the dispersion law, hydrodynamic nonlinearities of ions, and other effects may also play an important role. Systematic and consistent inclusion of all these effects with the aim of obtaining sufficiently simple improved dynamic equations adequately describing the final stage of collapse is impossible. Of course, the inclusion in the model (1) of specific effects (Landau damping,<sup>8,14</sup> the self-nonlinearities of the field, and the quasi-one-dimensional approximation,<sup>13</sup> saturation of nonlinearity, and ion kinetics<sup>15</sup>) carried out in a series of numerical experiments are of considerable interest. However, an adequate description of the general physical nature of the final stage of collapse is given only by the full system of kinetic equations

$$\begin{aligned} \frac{\partial f_e}{\partial t} + \mathbf{v} \frac{\partial f_e}{\partial \mathbf{r}} + \frac{e}{m} \nabla \varphi \frac{\partial f_e}{\partial \mathbf{v}} &= 0, \\ \frac{\partial f_i}{\partial t} + \mathbf{v} \frac{\partial f_i}{\partial \mathbf{r}} - \frac{e}{M} \nabla \varphi \frac{\partial f_i}{\partial \mathbf{v}} &= 0, \end{aligned} \quad (6)$$

$$\Delta \varphi = -4\pi e \int (f_i - f_e) d\mathbf{v}.$$

Moreover, it is the relatively short final stage of collapse of Langmuir cavitons in which the transfer of oscillation energy to electrons occurs that is of the greatest practical and scientific interest. Thus numerical modeling of the final stage of collapse taking into account the most important nonlinear and kinetic effects, i.e., solution of the kinetic equations (6) by the particle method, is of crucial importance. One can answer the important problems on the degree of anisotropy and caviton sizes at the final stage of their development, the time of caviton burnout, the fraction of energy transferred to the electrons, the distribution of accelerated particles, etc. only by use of such modeling.

Such research was recently carried out in two-dimensional geometry<sup>12,15</sup> in which, in the absence of previous work, a continuous calculation<sup>15</sup> and *a priori* inclusion of the most important effects of cavitons was realized. This provided a description of their evolution in a fairly wide inertial range and a conclusive picture of the final stage of two-dimensional collapse.

There are, however, serious reasons to consider that significant qualitative differences exist between two- and three-dimensional collapse.

1) It follows from Eq. (5) that in the three-dimensional case the level of HF energy grows considerably faster than the characteristic values of wave vectors of trapped oscillations and may exceed the thermal energy density in the process of evolution. This was demonstrated, for example, with calculations using averaged equations.<sup>8</sup> Large values of energy density may change the character of transfer of wave energy to particles, the character of electron acceleration, and the fraction of energy transferred to them.

2) It was shown in Refs. 12, 15 that a cessation of collapse and formation of quasi caviton structures was characteristic for two-dimensional weakly supercritical cavitons. In the three-dimensional case this phenomenon should be absent.

3) It follows from Eqs. (1) and (5) that the ratio of ion kinetic energy  $n_0 v_i^2 / 2$  to potential energy  $c_s^2 n_0 (\delta n / n_0)^2$

varies as  $(t_0 - t)^{4/d-2}$ . Thus in the three-dimensional case the ion kinetic energy grows faster than the potential energy and the density profile in the caviton is determined by ion inertia and not by thermal motion. Hence even if inclusion of additional nonlinear mechanisms in the final stage could stop collapse, the ion inertia should squeeze the caviton down to the point at which the electrons begin to interact with the oscillations. In this case the density depression will continue to deepen followed by burnout of a part of the plasmon energy. Thus density variations in three-dimensional cavitons could be significantly larger than in two-dimensional ones.

These discussions clearly illustrate the significance of solving the three-dimensional problem. In this work the final stage of evolution of three-dimensional cavitons is studied by the particle method. Such modeling is at the limit of possibilities of contemporary computer technology. A preliminary report on the results so obtained has been published.<sup>16</sup> Features of the numerical model and the organization of calculations are given in Refs. 18 and 19.

The three-dimensional kinetic calculations carried out provide a clear picture of collapse. In this case the caviton parameters, the density variations, and the maximum oscillation energies differ considerably from the corresponding results of two-dimensional calculations. The character of electron acceleration is different from that obtained in the two-dimensional case.

## 2. FORMULATION OF THE NUMERICAL MODEL

The difficulties of numerical modeling of the kinetics of Langmuir collapse have been repeatedly discussed in the literature.<sup>6,7,15,18</sup> The extremely large core requirements of the problem require careful consideration in the numerical model of *a priori* information on the physics of cavitons, on the one hand, and peculiarities in the computers used, on the other hand. In a series of calculations carried out with inadequate computational resources (see, for example, the three-dimensional calculation in Ref. 20 and the literature cited in Ref. 15) the physical properties of cavitons were not taken into account sufficiently, which led to inadequate modeling of the collapse of cavitons as a whole. We note some important factors.

1) An optimal choice of initial conditions is extremely important. Thus for the choice of a homogeneous initial ion distribution an initial fractionation of this distribution into localized cavitons occurs. This is accompanied by a drastic reduction in the efficiency with which the computational volume is used.

2) Excessively low particle mass ratios (for example,  $M/m \leq 25$ ) artificially reduce the role of ion inertia and lead to a compression of the inertial range.

3) The use of periodic boundary conditions is quite ineffective from the point of view of the expenditure of computational resources and (without taking special measures for the generation of the zero field harmonic) is physically incorrect for considering one caviton in the computational region. In this case due to the nonzero jump of the potential along the small axis of the dipole caviton there is an inevitable production of nonphysical cavitons, satellites, that spoil the characteristics and (when the resolution is inadequate) reduce the accuracy of the description of the basic caviton to an unacceptable level.

A physically correct and at the same time quite economical approach to the formulation of modeling the evolution of cavitons was proposed and executed in Refs. 12, 15, 16. In this case the properties of cavitons described above are exploited to the maximum extent. Suppose a dipole caviton is flattened along the  $z$ -axis. Then the electric field potential in it is antisymmetric along the dipole axis and symmetric in the perpendicular direction:

$$\begin{aligned} \varphi(x, y, z) &= \varphi(-x, y, z) = \varphi(x, -y, z) \\ &= \varphi(-x, -y, z) = -\varphi(x, y, -z). \end{aligned} \quad (7)$$

The symmetry properties allow us to consider only a portion of the caviton. For modeling three-dimensional cavitons by the particle method it is sufficient to carry out the calculation in the region

$$0 \leq x, y \leq L_{\perp}, \quad -L_z/2 \leq z \leq L_z/2, \quad \partial\varphi/\partial\mathbf{n}|_r=0, \quad (8)$$

containing a quarter of the caviton. A still greater gain can be achieved by solving the averaged equations (1), for which the region  $0 \leq x, y \leq L_{\perp}, 0 \leq z \leq L_z/2$  containing one-eighth of the caviton is sufficient with the subsidiary boundary condition  $\psi|_{z=0} = 0$ . Unfortunately, a corresponding boundary condition for particles is absent in particle models and the kinetic description must be carried out in region (8).

Because the minimum periodic spatial cell contains two complete cavitons in which the field changes in opposite phase, this formulation reduces the expenditure of computational resources for solving the averaged equations by a factor of 16 and for the particle method by a factor of 8 in comparison with the equivalent problem with periodic boundary conditions.

The optimal relation between linear region sizes is determined by the caviton anisotropy which depends on time and can become either larger or smaller than the initial value. Thus it is reasonable to take  $L_{\perp} = L_z = L$ , which corresponds to an initial anisotropy of order two. Such a value was observed approximately in the two-dimensional calculations<sup>12,15</sup> and in laboratory experiments.<sup>2</sup> In agreement with these considerations we carried out three-dimensional kinetic calculations in the cubic region  $0 \leq x, y \leq L, -L/2 \leq z \leq L/2$  containing a quarter of the caviton (Fig. 1) with reflection of particles at the boundaries where the normal component of the field is zero.

The initial conditions for the system (6) are clear. The distribution of particles should be Maxwellian with param-

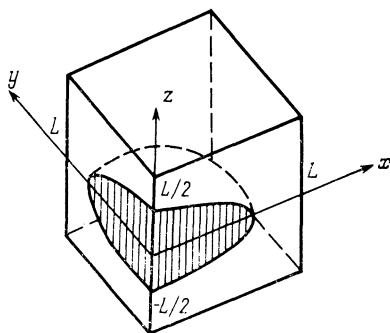


FIG. 1. The simulation region containing one-quarter of a caviton.

eters corresponding to a self-similar solution developing in the inertial range according to Eqs. (1). Simulations with such initial conditions, providing a preliminary solution of the averaged equations (1) which corresponds to a direct calculation, were carried out in two-dimensional geometry in Refs. 12, 15. Of course, for a computer with capacity approaching infinite size one can complete the establishment of a self-similar regime in the purely kinetic regime. However, first of all this is unrealistic for contemporary computer technology for multi-dimensional calculations and secondly, it is simply quite irrational in comparison with direct simulation. Even the continuous calculation is a quite time-consuming two-step simulation, especially in the three-dimensional case. Its performance should precede kinetic calculations of the final stage of collapse which are of independent interest. There is considerable arbitrariness in the initial conditions for solution of the pure kinetic problem, but they should satisfy some general requirements. Namely, the initial plasma state should contain small perturbations of ion density  $\delta n$  and charge density  $\rho = e\delta n$ :

$$n_i = n_0 + \delta n, \quad n_e = n_0 + \delta n + \widetilde{\delta n}, \quad (9)$$

initiating a density depression with HF filling for which the conditions of the description in the inertial range  $W/nT \ll 1, \delta n/n_0 \ll 1, kr_D \ll 1$ , and the condition for collapse (4) are satisfied.

With the aim of minimizing the effect of the superposition of frequencies and increasing the inertial range we chose the initial distribution of charge in the caviton as a combination of characteristic functions of the boundary problem

$$\Delta\varphi=0, \quad \frac{\partial\varphi}{\partial\mathbf{n}}\Big|_r=0, \quad 0 \leq x, y \leq L, \quad -L/2 \leq z \leq L/2$$

with a minimum value of the wave vector  $k = \pi/L$ :

$$\rho(\mathbf{r}) = \rho_0(1 + \cos kx)(1 + \cos ky)\sin kz. \quad (10)$$

The plasma density variation  $\delta n$  was given by the condition of gas kinetic and HF pressure balance

$$\frac{\delta n}{n_0}\Big|_{t=0} = -\frac{|\mathbf{E}|^2}{16\pi n_0 T_e} + C, \quad C = \frac{1}{16\pi n_0 T_e} \int |\mathbf{E}|^2 d\mathbf{r}, \quad (11)$$

where the constant on the right-hand side corresponds to the unavoidable vanishing of the integral in the region of density variation in particle models. The initial particle velocity distribution was taken as Maxwellian with the ion temperature and velocity equal to zero.

For the specified initial plasma state calculation of integrals (2) and (3) leads in dimensionless variables to

$$N = \frac{19}{6\pi} \rho_0^2 L^2, \quad H = (\rho_0/4)^2 [13.5 - 747(\rho_0/32\pi^2)^2 L^4]. \quad (12)$$

Here  $N$  and  $H$  are normalized by the total thermal energy  $L^3 n_0 T_e$ , the amplitude of the charge density  $\rho_0$ , and the length  $L$  described in units  $en_0$  and  $r_D$ , respectively. Then, supposing  $r_0 = L/2$  in the estimated condition (4) we have for the amplitude of the initial perturbation taking into account  $W/n_0 T_e \ll 1$

$$35.9/L^2 = \rho_0^{th} < \rho_0 \ll 4.99/L, \quad (13)$$

In the calculations we used the dipole particle method<sup>18,19,21,22</sup> employing fast Fourier transforms for finding the field on the grid of  $33^3$  points. The choice of linear size  $L$  was made as a reasonable compromise between the requirement of a sufficiently broad (for heavy ion acceleration) inertial range and the limitations of using the EC-1037-EC-2706 multiprocessor computer facility of the Institute of Space Research.<sup>18</sup> For the standard linear size of a cell  $\Delta = r_D$  the size of the computational region was  $L = 32 r_D$ . However, taking into account that according to the results of two-dimensional calculations and laboratory experiments the minimum caviton size is quite large [ $l_{\min} \sim 10 r_D$  (Refs. 12, 15),  $l_{\min} \sim 20 r_D$  (Ref. 2)], we used a coarser grid with  $\Delta = 2r_D$ . In this case the dipole method was modified: an unconventional smoothing was used in  $k$ -space, also correcting wave dispersion in the long wavelength part of the spectrum.<sup>19</sup> Thus, in effect the whole caviton was modeled in the regions  $64 \times 64 \times 32 r_D^3$  ( $L = 32 r_D$ , standard method) and  $128 \times 128 \times 64 r_D^3$  ( $L = 64 r_D$ , modified method).

The particle mass ratio was taken to be quite large:  $100 \leq M/m \leq 400$ , and the general number of modeled particles was  $\sim 1.8 \times 10^6$ . The control of the correctness of the calculations was the total energy in the system: nonconservation of total energy was less than several percent. Moreover, at the initial stage of caviton evolution (for small levels of long wavelength oscillations) we always have strict conservation of the total field energy.

### 3. RESULTS OF CALCULATIONS AND THEIR EVALUATION

We note that for all simulation cases the coordinates of the maximum of the HF field corresponded with the coordinates of the minimum of the ion density depression in the process of evolution and coincided with their initial position

(initial coordinate). The initial series of calculations carried out for a region of size  $L = 32 r_D$  demonstrated a picture of collapse such that the maximum intensity of the HF field grew  $\sim 2$  times, accompanied by a deepening of the ion depression by  $\sim 1.5$  times. However, the narrowness of the inertial range due to the small size of the initial perturbation led to rapid absorption of the average energy of HF oscillations by electrons due to inclusion of Landau damping.

Significant progress was made by doubling the linear region size  $L = 64 r_D$ . The collapse threshold measured experimentally according to the amplitude of the initial density perturbation  $\rho_0^* = 0.009$  practically coincided with the one calculated from Eq. (13) for which  $\rho_0^{\text{th}} = 0.0088$ . For values  $\rho_0 > \rho_0^*$  focusing of the field in the center of the initial density perturbation was observed along with deepening of the ion depression leading to burnout of the energy of HF oscillations (the spatial distributions of fixed caviton characteristics for one of the typical variants is given in Fig. 2). A choice of perturbation amplitude  $\rho_0 < \rho_0^*$  led to destruction of the initial field and density distribution. It is convenient to introduce as was done in two-dimensional calculations<sup>12,15</sup> a supercriticality parameter  $\varepsilon = W(\rho_0)/W(\rho_0^*) = (\rho_0/\rho_0^*)^2$  equal to the increase of initial intensity over the threshold intensity for collapse. Below we present results of calculations for which the energy density of the initial distribution of the HF field in the center of the caviton varied from  $0.135 \leq W_{\max}/n_0 T_e \leq 0.485$ ; the average value of the HF field energy in the region varied in the range  $0.024 \leq W/n_0 T_e \leq 0.080$ .

The time dependence of the average energy of the HF oscillations  $W/n_0 T_e$ , the maximum energy of the HF oscillation  $W_{\max}/n_0 T_e$ , and the depression depth  $(n_{\max} - n_{\min})/n_0$  for four model variants corresponding to var-

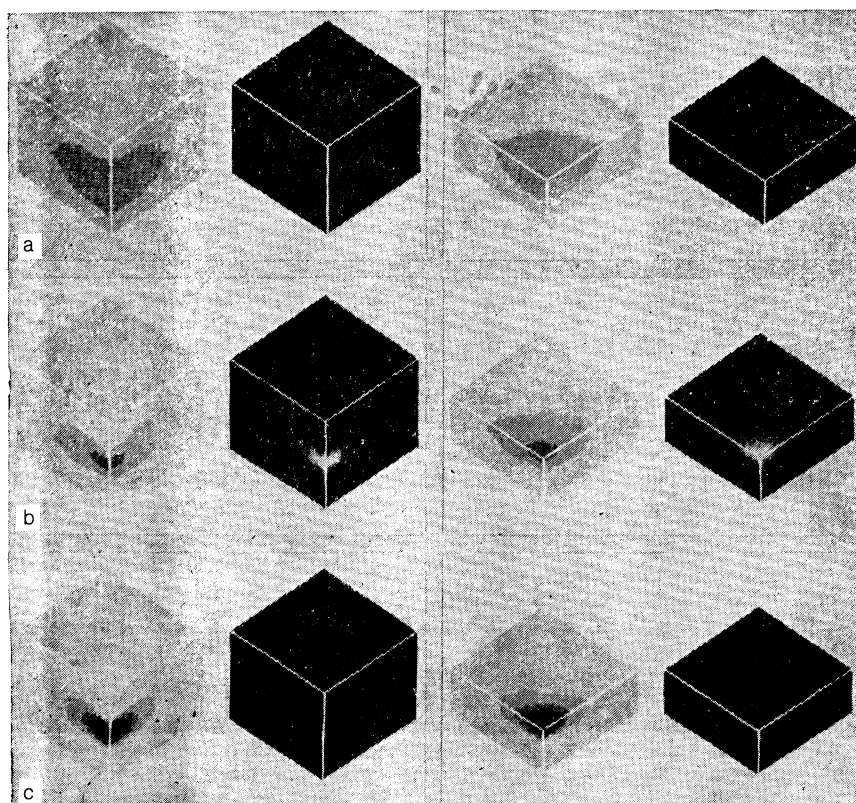


FIG. 2. Spatial distribution of HF field energy density  $E^2/8\pi n_0 T_e$  (dark parallelipeds) and the ion density  $n_i/n_0$  (light parallelipeds) for the case  $\rho_0 = 0.015$  and  $M/m = 400$ ; (a) initial condition, (b) time of field maximum in the caviton ( $t = 139.2 \omega_p^{-1}$ ), and (c) time of maximum caviton depth ( $t = 284.0 \omega_p^{-1}$ ). On the left is the whole region and on the right is a cross-section through the  $z = 0$  plane.

ious values of physical parameters are presented in Fig. 3. In cases of large increases over the threshold values  $\rho_0 = 0.02$ ,  $\varepsilon = 5$  and  $M/m = 100$  (Fig. 3, curve 1), and  $\rho_0 = 0.15$ ,  $\varepsilon = 3$ , and  $M/m = 100$  (Fig. 3, curve 2), a clear picture of collapse is observed with growth of field energy at the maximum by approximately 6 times (to  $W_{\max}/n_0 T_e \sim 3$ ), deepening of the ion depression by 3–5 times (to  $n_{\max} - n_{\min})/n_0 \sim 0.7$ ), and absorption of a significant part ( $\sim 70\%$ ) of the HF oscillation energy with characteristic dissipation time  $\cong 8-9 \omega_{pi}^{-1}$ . In the two-dimensional case<sup>12,15</sup> in the supercritical region  $2 < \varepsilon < 6$  a “prolonged” regime of collapse occurred and the regime of “clear” collapse occurred only for  $\varepsilon > 6$ . Even in the case of the near-threshold regime  $\rho_0 = 0.01$ ,  $\varepsilon = 1.1$  and  $M/m = 100$  (Fig. 3, curve 4) we observed after a time  $\sim 30 \omega_{pi}^{-1}$  a growth of field energy at the maximum of approximately 3 times and a deepening of the density depression more than 2 times; the average oscillation energy was not changed. In the two-dimensional case for  $\varepsilon$  exceeding 1.25 at the same times the formation of a caviton structure took place.<sup>15</sup>

In order to clarify the role of ion inertia for amplitude  $\rho_0 = 0.015$  the calculations were carried out twice, for  $M/m = 100$  and 400. Comparison of the temporal dependences of basic caviton characteristics for these cases on an ion time scale (with argument  $\omega_{pi} t$ ) showed that the curves approximately coincide with a shift in time by  $\sim 4-5 \omega_{pi}^{-1}$  due to ion immobility at the initial moment of time; the burnout time in units  $\omega_{pi}^{-1}$  did not depend on the mass ratio  $M/m$ . This provides a means of generalizing the modeling results to a real mass ratio.

Consistent with qualitative ideas about the role of ion inertia in the three-dimensional case for the clear collapse cases the basic deepening of the ion density depression occurred after the HF field reached its maximum (see Fig. 3 and also Fig. 2 of the short note<sup>16</sup>). The levels of HF energy and plasma density variations reached exceed considerably (by more than a factor of two) those observed in the analogous two-dimensional calculations.<sup>12,15</sup>

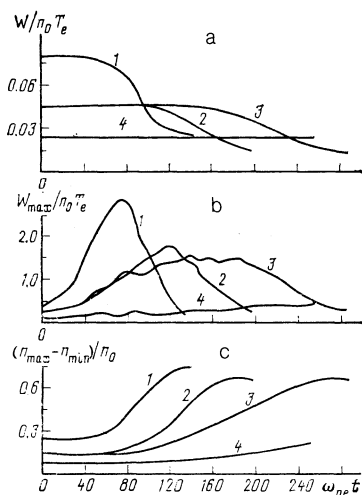


FIG. 3. Temporal dependence of characteristics of the collapsing caviton: (1)  $\rho_0 = 0.020$  and  $M/m = 100$ ; (2)  $\rho_0 = 0.015$  and  $M/m = 100$ ; (3)  $\rho_0 = 0.015$  and  $M/m = 400$ ; (4)  $\rho_0 = 0.010$  and  $M/m = 100$ . Part (a) is the average energy  $W/n_0 T_e$  of the HF field in the caviton; (b) is the maximum field energy  $W_{\max}/n_0 T_e$  in the caviton; and (c) is the overall maximum value of the caviton depth  $(n_{\max} - n_{\min})/n_0$ .

Analysis of the spatial dependences of field intensity and density variations along and perpendicular to the dipole axis showed that in the process of caviton collapse the oblate form is preserved with a tendency to some flattening. Thus for the case  $\rho_0 = 0.15$ ,  $\varepsilon = 3$ , and  $M/m = 400$  the anisotropy (ratio of the large caviton dimension to the small one) at characteristic times  $t_1 = 0$ ,  $t_2 = 139.2 \omega_p^{-1}$  (time of field maximum), and  $t_3 = 284 \omega_p^{-1}$  (time of maximum density deformation) was 1.65, 2.1, and 2.3 for field intensity and 1.65, 2.3, and 2.2 for density depressions, respectively.

An important result observed for all clear collapse cases is the large ( $\sim 14-16 r_D$ ) minimal caviton size which in two-dimensional geometry reached a value  $\sim 10 r_D$  (Refs. 12, 15). This result agrees with the data of laboratory experiments<sup>2</sup> which previously seemed difficult to explain. The explanation is that due to the higher level of  $W_{\max}/n_0 T_e$  in comparison to the two-dimensional situation the interaction of electrons with oscillations is considerably modified by the strong nonlinearity. This supposition is also supported by the analysis presented in Fig. 4 of the  $(z, v_z)$  phase plane ( $z$  is the direction of field oscillations with the pattern averaged in the perpendicular direction) in which the presence of vortices is clearly traced which indicate wave-breaking in the caviton. The final electron velocity distribution (see Fig. 3 of Ref. 16) is characterized by considerable anisotropy (the maximum electron acceleration occurs along the dipole axis) and the presence of strongly accelerated electrons to  $v = v_{\max} = 9 v_{Te}$  [in the two-dimensional calculations  $v_{\max} \cong 5 v_{Te}$  (Ref. 15)]. This means, in particular, that collapse is a more effective method of generating fast electrons than one could have expected on the basis of the model two-dimensional calculations.

We present in Fig. 5 the fraction of the total number of electrons whose speed exceeds 3, 5, and  $7 v_{Te}$  as a function of time. One can see that the energy of HF oscillations is transferred to a small fraction (about 0.3% of the total number) of the electrons in the tail of the distribution. Initially the growth of the number of accelerated particles corresponds to the attainment of the HF field maximum which evidences the cessation of collapse with the beginning of effective electron acceleration.

The results obtained in three-dimensional kinetic modeling are a high level of the local values of HF oscillation

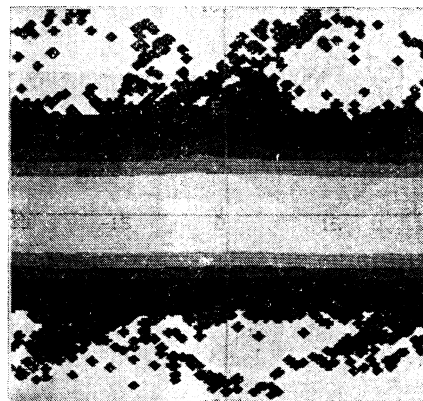


FIG. 4. Electron phase space  $(z, v_z)$  (pattern averaged in the perpendicular direction) for the case  $M/m = 400$  and  $\rho_0 = 0.015$  at  $t = 284 \omega_p^{-1}$ .

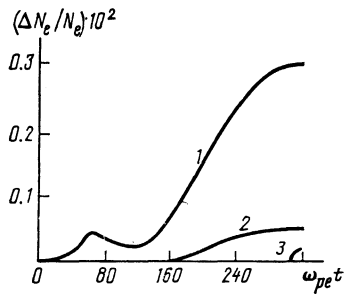


FIG. 5. Time dependence of the fraction of the total number of electrons whose speed exceeds (1)  $3 v_{Te}$ ; (2)  $5 v_{Te}$ ; (3)  $7 v_{Te}$  for the case  $\rho_0 = 0.015$  and  $M/m = 400$ .

energy, a quasi-one-dimensional tail of the electron distribution function, and caviton flatness. These make subsidiary one-dimensional calculations attractive for a qualitative analysis of the general physical picture of the final stage of collapse which follow the burnout of structures with large values of HF energy over ion density depressions by the particle method. We note that kinetic calculations of the evolution of one-dimensional waves of large amplitude were carried out, for example, in a series of papers of Buchel'nikova and co-authors (see, for example, Ref. 23). In contrast to these papers we studied the process of damping of the distribution obtained as a result of the three-dimensional evolution. The subsidiary one-dimensional calculations were carried out for simplicity with periodic boundary conditions, i.e., two cavitons with fields in opposite phase were considered.

This field structure in cavitons was modeled by an initial distribution of soliton type:

$$E(x) = E_0 [1/\text{ch } \lambda(x - 1/4L) - 1/\text{ch } \lambda(x - 3/4L)] \quad (14)$$

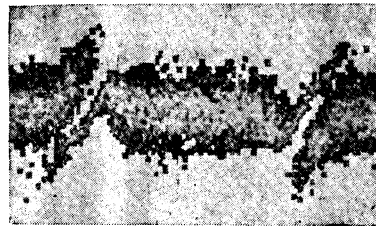


FIG. 7. Electron phase space for  $t = 4.8 \omega_p^{-1}$  in the one-dimensional experiment.

with parameters ( $L$  is the length of the region,  $E_0$  is the amplitude, and  $\lambda$  is the inverse size) corresponding to parameters of the three-dimensional caviton at the initial moment of field burnout. The value of ion density deformation was determined by balancing high frequency and gas kinetic pressures

$$\alpha \frac{E^2}{16\pi n_0 T_e} = -\frac{\delta n}{n_0} + C, \quad C = \frac{\alpha}{16\pi n_0 T_e} \int_0^t E^2 dx,$$

where  $\alpha$  is a coefficient allowing one to select the necessary value of the depth of the ion density depression for a given field amplitude.

After assigning as initial conditions the caviton parameters  $W_{\max}/n_0 T_e = 1.8$ ,  $-\delta n/n_0 \cong 0.5$ , and the depression half-width  $15 r_D$ , corresponding to the three-dimensional case  $\rho_0 = 0.015$ ,  $\varepsilon = 3$ , and  $M/m = 400$ , we observed rapid (2-3 plasma periods) burnout of this structure accompanied by the formation of a tail of accelerated particles of the electron distribution function; the profile of the ion depression during this time remained practically unchanged (Fig. 6). On the phase plane corresponding to this case one can see the formation of features with successive excitation of multi-

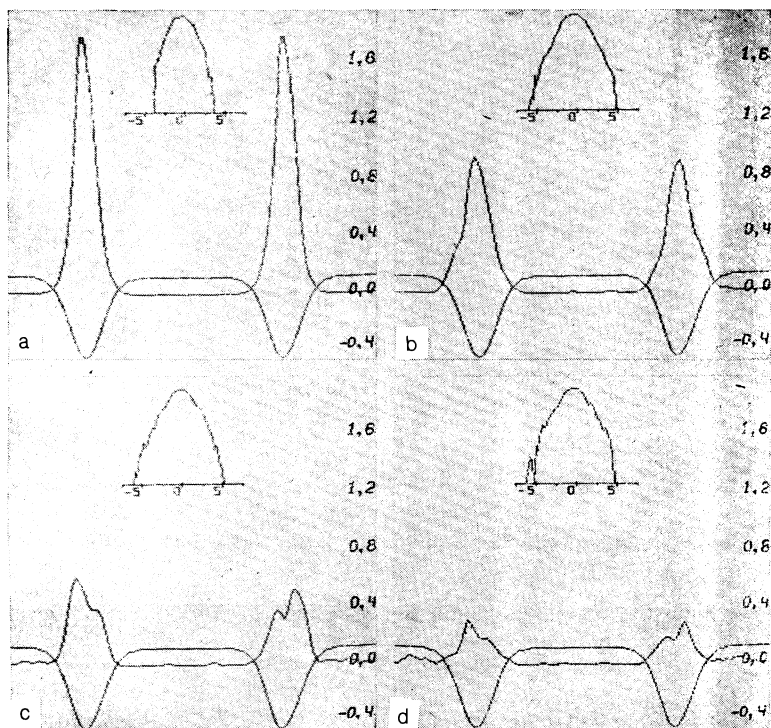


FIG. 6. Spatial dependences of the oscillation energy density  $E^2/8\pi n_0 T_e$ , density variation  $\delta n/n_0$ , and electron distribution function (above) in the one-dimensional experiment: (a)  $t = 0$ ; (b)  $t = 6.4 \omega_p^{-1}$ ; (c)  $t = 12.8 \omega_p^{-1}$ ; and (d)  $t = 19.2 \omega_p^{-1}$ .

streaming (Fig. 7). Calculation of the case with zero temperature electrons and the same initial conditions (whose phase space evolution is presented in Fig. 8) gave an even clearer picture of the excitation of multi-streaming.

The physical process of energy transfer to electrons is the following. The electric field of the caviton changes direction during a time  $\tau \sim \pi/\omega_p$ . If a significant number of electrons succeeds in traveling through the caviton during this time, they carry away a significant part of the energy lost by the waves. In our numerical calculations the electric field of the oscillations is so large that even the initially stationary particles can be accelerated and leave the caviton during the time  $\tau$ . In this case part of the particles are reflected back and create a multi-streaming motion which can be seen clearly in Fig. 7. Finite temperature blurs the pattern, but the basic features in phase space appear fairly well.

Similar behavior of the phase space is displayed in three-dimensional modeling. The absence of a break in the region of small velocities is explained by the fact that the pattern shown in Fig. 4 is averaged in the perpendicular direction and particles from the periphery of the caviton where the field is small fill the break. We also note that the burnout energy fraction in the one-dimensional calculations was about 80% which agrees well with the 70% burnout in the three-dimensional modeling.

With increase of the initial size of the caviton, transfer of energy to particles decreases sharply which also leads to a decreased level of the HF field in the caviton. To model this effect we take into account that in the real three-dimensional

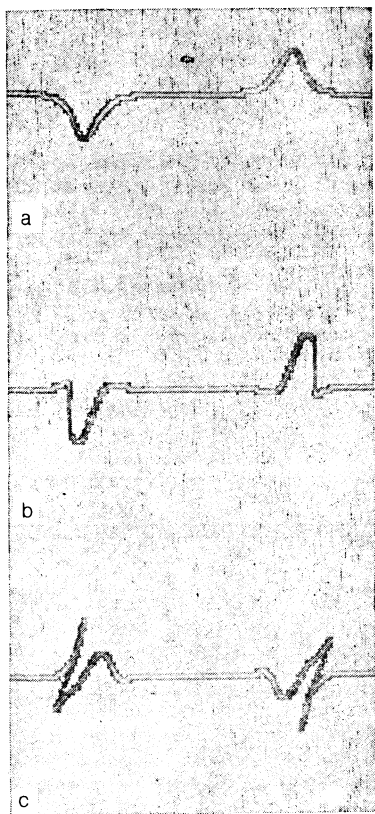


FIG. 8. Phase space evolution in the one-dimensional experiment for  $T_e = 0$ : (a) the initial state ( $t = 1.2 \omega_p^{-1}$ ), (b) wave breaking ( $t = 3.2 \omega_p^{-1}$ ), and (c) multi-streaming ( $t = 6.0 \omega_p^{-1}$ ).

situation, until absorption of HF energy caviton begins, collapse occurs with conservation of plasmon number  $N \sim W_{\max} l^3$ , where  $l$  is the characteristic size and  $W_{\max}$  is the maximum value of HF energy in the caviton. Thus the scales  $r_1$  and  $r_2$ , corresponding to  $W_{1\max}$  and  $W_{2\max}$ , are connected by the relation  $r_2 = r_1 (W_{1\max}/W_{2\max})$ . This provides a means of modeling damping of such a caviton at an earlier stage. For the previously considered example  $W_{2\max}/n_0 T_e = 1.8$  and  $r_2 = 15 r_D$ , the scale  $r = 24 r_D$  corresponds to the value  $W_{\max}/n_0 T_e = 0.5$ . Calculation of the case with initial conditions  $W_{\max}/n_0 T_e = 0.5$  and  $r = 24 r_D$  shows a practically unchanged energy content in the caviton over several plasma periods. This emphasizes the threshold character of the HF energy burnout process with the amplitude of the field and the size of its localization.

#### 4. CONCLUSION

Study of the final stage of evolution of three-dimensional Langmuir cavitons by the particle method demonstrated a clear collapse picture. The basic characteristics of cavitons and their interaction with electrons, maximum levels of HF energy, ion density deformation amplitude, limiting electron velocity, and minimum final caviton size considerably exceed the analogous values obtained in two-dimensional kinetic calculations. The geometrical characteristics of cavitons, the large minimum size ( $\sim 16 r_D$ ) and the degree of anisotropy agree with those observed experimentally.<sup>2</sup> Burnout of the high intensity structures is accompanied by formation of vortices in phase space, the production of multi-streaming, and the ejection of a significant fraction of particles from the caviton.

We note that observation in the stable case of a large minimum caviton size means, in particular, that one of the most important caviton parameters, the characteristic wave vector of trapped oscillations, remains small ( $kr_D \sim 0.2$ ) to the end of the evolution. This circumstance may be important for constructing a simplified description of collapse. On the other hand, the large value of the minimum caviton size may mean that in real plasma experiments the inertial range, the ratio of initial to final caviton sizes, is not too large. It is necessary to take this into account in interpreting the experiments.<sup>24</sup>

In a series of papers (see Ref. 25 and the literature cited there) attention was drawn to initiation of collapsing cavitons, i.e., formation of new cavitons predominantly in the places of burned-out ones. This phenomenon depends considerably on the structure of the density depression formed at the location of the burned-out caviton. Two-dimensional modeling was carried out in Ref. 25 using dynamic equations. Our calculations indicate a significant difference in  $\delta n$  profiles for two- and three-dimensional calculations. The large value of density variation makes a dynamic description of  $\delta n$  inapplicable which should be taken into account in modeling of turbulence.

We modeled the final stage of collapse with fairly arbitrary initial conditions. Performance of a three-dimensional continuous calculation is undoubtedly of interest. We hope that this problem will be solved in the near future.

The authors are grateful to A. I. Dyachenko for interest in the work and help with the correction of the dipole particle method, and also to I. B. Petrov for participation in the programming.

- v. E. Zakharov, Zh. Eksp. Teor. Fiz. **62**, 1745 (1972) [Sov. Phys. JETP **35**, 908 (1972)].
- <sup>2</sup> A. Y. Wong and P. Y. Cheung, Phys. Rev. Lett. **52**, 1222 (1984). Phys. Fluids **28**, 1538 (1985).
- <sup>3</sup> V. E. Zakharov, in *Basic Plasma Physics*, A. A. Galeev and R. N. Sudan, eds., Vol. 2 (North Holland, Amsterdam, 1984).
- <sup>4</sup> V. D. Shapiro and V. I. Shevchenko, in *Basic Plasma Physics*, A. A. Galeev and R. N. Sudan, eds., Vol. 2 (North Holland, Amsterdam, 1984).
- <sup>5</sup> M. V. Goldman, Rev. Mod. Phys. **56**, 709 (1984).
- <sup>6</sup> A. M. Rubenchik, R. Z. Sagdeev, and V. E. Zakharov, Comm. Plasma Phys. Contr. Fus. **9**, 183 (1985).
- <sup>7</sup> S. I. Anisimov, M. A. Berezovskii, V. E. Zakharov *et al.*, Zh. Eksp. Teor. Fiz. **84**, 2046 (1983) [Sov. Phys. JETP **57**, 1192 (1983)].
- <sup>8</sup> L. M. Degtyarev, V. E. Zakharov, R. Z. Sagdeev *et al.*, Zh. Eksp. Teor. Fiz. **85**, 1221 (1983) [Sov. Phys. JETP **58**, 710 (1983)].
- <sup>9</sup> M. A. Mal'kov, R. Z. Sagdeev, V. D. Shapiro, and V. I. Shevchenko, *Nonlinear and Turbulent Processes in Physics*, ed. R. Z. Sagdeev, Harwood Academic, 1983, p. 405.
- <sup>10</sup> V. M. Malkin, Zh. Eksp. Teor. Fiz. **87**, 433 (1984) [Sov. Phys. JETP **60**, 248 (1984)]; Zh. Eksp. Teor. Fiz. **90**, 59 (1986) [Sov. Phys. JETP **63**, 34 (1986)].
- <sup>11</sup> M. B. Isichenko and V. V. Yan'kov, Fizika Plazmy **12**, 169 (1986) [Sov. J. Plasma Phys. **12**, 98 (1986)].
- <sup>12</sup> A. I. Dyachenko, V. E. Zakharov, A. M. Rubenchik, R. Z. Sagdeev, and V. F. Shvets, Pis'ma Zh. Eksp. Teor. Fiz. **44**, 504 (1986) [JETP Lett. **44**, 648 (1986)].
- <sup>13</sup> V. L. Galinskii, M. A. Mal'kov, and G. I. Solov'ev, Fizika Plazmy **13**, 1269 (1987) [Sov. J. Plasma Phys. **13**, 733 (1987)].
- <sup>14</sup> P. A. Robinson, D. L. Newman, and M. V. Goldman, Phys. Rev. Lett. **61**, 702 (1988).
- <sup>15</sup> A. I. Dyachenko, V. E. Zakharov, A. M. Rubenchik, R. Z. Sagdeev, and V. F. Shvets, Zh. Eksp. Teor. Fiz. **94**, 144 (1988) [Sov. Phys. JETP **67**, 513 (1988)].
- <sup>16</sup> V. E. Zakharov, A. N. Pushkarev, A. M. Rubenchik, R. Z. Sagdeev, and V. F. Shvets, Pis'ma Zh. Eksp. Teor. Fiz. **47**, 239 (1988) [JETP Lett. **47**, 287 (1988)].
- <sup>17</sup> V. E. Zakharov, Usp. Fiz. Nauk **155**, 529 (1988) [Sov. Phys. Usp. **31**, 672 (1988)].
- <sup>18</sup> A. Yu. Golovich, A. N. Pushkarev, R. Z. Sagdeev, V. F. Shvets, and V. I. Shevchenko, Preprint IKI No. 1347, Moscow, 1988.
- <sup>19</sup> A. I. Dyachenko, A. N. Pushkarev, A. M. Rubenchik, and V. F. Shvets, Comput. Phys. Commun., 1989 (in press).
- <sup>20</sup> A. N. Polyndov, B. D. Selyandin, and Yu. S. Sigov, Dok. Akad. Nauk SSSR **246**, 58 (1979) [Sov. Phys. Dokl. **24**, 352 (1979)]; preprint IPM No. 145, Moscow, 1978.
- <sup>21</sup> R. Hockney and J. Eastwood, *Computer Simulation Using Particles*, McGraw-Hill, New York, 1981 (Russ. Transl., Mir, Moscow, 1987).
- <sup>22</sup> M. A. Berezovskii, M. F. Ivanov, I. V. Petrov, and V. F. Shvets, Programming, No. 6, p. 37 (1980) (in Russian).
- <sup>23</sup> N. S. Buchel'nikova and E. P. Matochkin, Preprint IYaF No. 155, Novosibirsk, 1986.
- <sup>24</sup> D. M. Karlidov, A. M. Rubenchik, K. F. Sergeichev, and I. A. Sychev, Phys. Lett. A, 1989 (in press).
- <sup>25</sup> D. Russel, D. F. DuBois, and H. A. Rose, Phys. Rev. Lett. **60**, 581 (1988).

Translated by D. F. Smith